ELSEVIER

Biophysical Chemistry 57 (1995) 93–102

Biophysical Chemistry

Crowding-induced organization of cytoskeletal elements. III. Spontaneous bundling and sorting of self-assembled filaments with different flexibilities

Daniel T. Kulp, Judith Herzfeld *

Department of Chemistry Brandeis University Waltham, MA 02254-9110, USA

Abstract

The typical cell contains ca. 25 vol.-% protein, of which ca. 10% forms cytoskeletal filaments and ca. 90% is non-aggregating globular protein [1]. It has previously been theoretically predicted that, under such highly crowded conditions, rigid filaments will coalesce into tight bundles coexisting with an isotropic solution of globular proteins [2]. In the present work we show that such spontaneous bundling will occur even when filament flexibility is taken into account because the persistence length of the filaments is much longer than the diameter of the globular proteins. The theoretical results are consistent with experimentally observed bundling of F-actin (the most flexible of the three most common types of cytoskeletal filaments) in the presence of globular macromolecules [3,4]. The main effect of increased filament flexibility on bundling is to cause somewhat looser packing. In mixtures of filaments, differences in flexibilities can lead to segregation. This segregation is accentuated when the stiffer filament is also wider. The results suggest that actin filaments and microtubules will spontaneously form segregated bundles in the presence of cellular concentrations of globular proteins. While cross-linking proteins may serve to stabilize these bundles, their more important function in bundling may be to fine tune the structure (e.g., polarity and registration of filaments).

Keywords: Statistical thermodynamics; Cytoskeleton; Bundles; Actin; Microtubules; Excluded volume; Flexibility

1. Introduction

The cytoskeleton is an organized system of protein filaments that plays an important role in cell morphology, rheology, motility, division and intracellular transport. Unlike the large mineralized skeleton of vertebrate animals, the cytoskeleton is dynamic, with components constantly disassembling and reassembling in new arrangements throughout the cell. Control of these processes is vital for normal cell behavior and defects in control can result in pathology.

A variety of filament binding proteins have been identified and implicated in the control of cytoskeletal organization. However, in order to clearly define the influence of particular binding proteins, it is necessary to understand the behavior of cytoskeletal filaments in the absence of binding proteins. The

* Corresponding author.

SSDI 0301-4622(95)00050-X

usual assumption is that free filaments will be randomly dispersed in solution to maximize the entropy. However, in highly crowded solutions, where packing constraints are severe, an isotropic dispersion is not necessarily the state of maximum entropy. Due to excluded volume, there are trade-offs between the entropies associated with different spatial degrees of freedom. In particular, at sufficiently high concentrations, the rotational freedom lost by orientational ordering of elongated particles is exceeded by the translational entropy gained, so that an orientationally ordered state is more stable than the isotropic state [5]. At still higher concentrations, translational entropy lost due to positional ordering in some dimensions may be more than compensated by translational entropy gained in other dimensions so that positional ordering in successive degrees (smectic, columnar or crystalline) occurs spontaneously [6,7]. Separation can also occur, in which the entropy lost by particles in one phase is exceeded by the entropy gained by the particles in the other. Thus under the highly crowded conditions that prevail in cells (20–30 vol.-% protein), non-ideality can lead not only to the well-known quantitative exaggeration of ordinary behavior described by non-unitary activity coefficients, but also to qualitatively different phenomenology in the form of long-range, entropically-driven spatial order.

In order to describe excluded volume effects in detail, so as to determine what behavior can be expected of cytoskeletal elements under crowded conditions, it is necessary to use statistical thermodynamics. The theory must take into account that, in addition to rotational and translational degrees of freedom, cytoskeletal systems have degrees of freedom associated with the reversible self-assembly of filaments. Thus, in order to fully describe these systems, it is necessary to consider aggregate size distributions, as well as their orientation and position distributions. For several relatively well-studied reversibly assembling systems, we have shown that the experimentally observed behavior at high concentrations can be understood in terms of the balance between free energy contributions due to favorable contacts between monomers (which drive aggregation), the ideal entropy of mixing (which tends to broaden particle size, orientation and position distributions), and interparticle interactions, including excluded volume (which drives positional and orientational ordering, as described above) and soft repulsions (which oppose alignment) [8]. For polyaromatic compounds that stack to form cylindrical aggregates the theory successfully reproduced the experimentally observed concentration and temperature dependence of isotropic, nematic and columnar order, including the presence of a triple point where all three phases coexist. In addition, the calculated mean aggregate length compared well with experiment. For perfluorinated surfactants which form disk-shaped micelles, the theory reproduced the experimentally observed concentration and temperature dependence of isotropic, nematic and smectic order, again including the presence of a triple point. The calculated average micelle diameter agreed qualitatively with that determined experimentally.

The success of the theory for the relatively well-characterized binary systems (solvent and one self-assembling solute) lends confidence that the theoretical approach is sound and can be extended to ternary systems (solvent and two solutes) to model the behavior of cytoskeletal proteins in the presence of other proteins. For mixtures of filament forming protein and globular protein, at the concentrations found in cells, the theory predicts that filaments will not only align but also spontaneously coalesce into dense bundles that coexist with an isotropic solution containing the globular protein [2]. This phenomenon occurs because a great deal of space is wasted when round particles are interspersed between rod-shaped particles. At high concentrations, when space is scarce, entropy is actually gained upon demixing and the greatest entropy is achieved when most of the solvent stays with the smaller round particles. This spontaneous filament bundling, has been seen experimentally in mixtures of F-actin and high molecular weight globular molecules [3,4]. Madden and Herzfeld [9] have also considered the effect of capping proteins. The results indicate that by decreasing the filament lengths, capping proteins make it easier for filaments to mix with globular protein and thereby reduce the tendency to form tight bundles.

In these studies of cytoskeletal systems, filaments were approximated as perfectly rigid rods. However, cytoskeletal filaments are somewhat flexible and the internal orientational entropy permitted by this flexibility may resist the alignment of filaments in tight

bundles. The persistence length (P_L = the decay length for the correlation between the orientations of segments along the filament) is approximately 6000 nm for actin microfilaments [10]. It is known that when the length of a fiber is one-tenth its persistence length then the particles no longer behave as rigid [11]. Therefore it is necessary to include flexibility in any study of F-actin.

Khokhlov and Semenov (KS) were the first to study the intraparticle orientational entropy due to filament flexibility [12,13]. Several other researchers [14–17] extended the KS model to explain the high concentration behavior of solutions of semi-flexible molecules (e.g., poly-γ-benzyl-L-glutamate, poly(hexyl isocyanate), and schizophyllan). They have found that the theory reproduces the experimental data for these monodisperse systems. The theory has also been applied to reversibly self-assembling systems by making the stringent assumption of a narrow aggregate size distribution [18]. Here we allow an arbitrarily broad size distribution and make the weaker assumption that most of the filaments are long enough that the orientation distribution of filament segments is independent of filament length. This approximation is justified because filament assembly is highly cooperative which keeps the population of short filaments very low. Using this approach we consider two types of ternary solutions: a filament forming protein mixed with a non-aggregating globular protein, and mixtures of two filament forming proteins with different flexibilities.

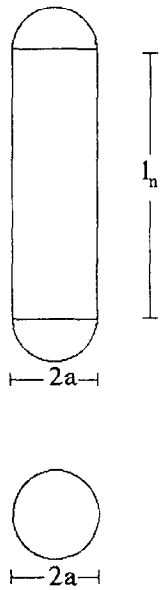

Fig. 1. Schematic of the model particles. In this model, n spherical monomers of radius a reversibly self-assemble to form an aggregate of the same radius and length $l_n = (4a/3)(n-1)$.

2. Model

The overall approach is to calculate the dependence of the free energy on the size and orientation distributions of the particles and to determine the equilibrium state by minimization of the free energy with respect to these distributions. (As in previous modeling of cytoskeletal systems, the further possibility of positional ordering is neglected due to the absence of relevant experimental observations.) The key to the modeling is therefore a good representation of the contributions to the free energy. These may be divided into three categories: contributions due to the assembly of a polydisperse population of particles, contributions due to the orientational entropy of the particles, and contributions due to interactions between particles. The total free energy is therefore given by the sum

$$F_{tot} = F_{pop} + F_{orient} + F_{inter} \quad (1)$$

In order to deal exclusively in intensive variables, it is convenient to work with the unitless free energy density,

$$f_{tot} = \beta F_{tot}/V = f_{pop} + f_{orient} + f_{inter} \quad (2)$$

where $\beta = 1/kT$ and V is the total volume.

2.1. The population of particles

As before, we model monomers as spheres, and filaments as arbitrarily long spherocylinders of the same diameter, formed by the linear self assembly of monomers (see Fig. 1). This simplified geometry captures the essence of open-ended self-assembly and is therefore an adequate generic model of cytoskeletal filaments. In the future, it will be interesting to compare the behavior of more detailed models that reflect the specific multi-stranded geometries of different cytoskeletal filaments with the present generic case, in order to understand the functional

significance of the variations. However, at this time we are more interested in what the various cytoskeletal systems have in common than in how they differ.

The free energy due to the linear aggregation of monomers of type j into filaments is described phenomenologically by assigning an energy of $\phi_{j0}kT$ to each contact. To incorporate cooperativity, an additional term is introduced which is conceptualized as the free energy required for a monomer to assume the conformation appropriate for aggregation, $\phi_{jc}kT$. Thus,

$$f_{\text{assoc}} = -\sum_{j,n>1} c_{jn}\left[\phi_{j0}(n-1) - n\phi_{jc}\right] \tag{3}$$

where c_{jn} is the number concentration of particles composed of n monomers of type j. Rearranging the terms gives

$$f_{\text{assoc}} = -\sum_{j,n>1} \left[(\phi_{j0} - \phi_{jc})(n-1) - \phi_{jc}\right] \tag{4}$$

so that, in effect, aggregate growth is driven by a net free energy of $(\phi_0 - \phi_c)kT$ per monomer added, while an end penalty of $\phi_c kT$ is responsible for cooperativity. The polydispersity of the resulting population contributes an additional free energy due to mixing of

$$f_{\text{mix}} = \sum_{j,n} c_{jn}\left(\ln\left(c_{jn}\Lambda_j^3\right) - 1\right) \tag{5}$$

where Λ_j is the thermal wavelength of the monomer. The overall free energy due to the assembly of a polydisperse population of particles is thus given by

$$f_{\text{pop}} = f_{\text{assoc}} + f_{\text{mix}} \tag{6}$$

2.2. Orientational entropy

Khokhlov and Semenov formulated a systematic expression for the free energy due to the orientational entropy of semi-flexible fibers in terms of the orientation distribution function $g(n(t))$, where $n(t)$ is a tangential unit vector at position t along the fiber contour [12,13]. Unfortunately, this leads to an expression which is too complex for specific calculations, so KS examined the two extremes of the fiber length L: $L/P_L \ll 1$, which is the limit of rigid rods, and $L/P_L \gg 1$, which is the worm-like limit. In these limits, the orientational free energy per particle is given by

$$\sigma_p = \int g(\Omega)\ln g(\Omega)\,\mathrm{d}\Omega + \frac{L}{12P_L}\int\left[\nabla g(\Omega)\right]^2 / g(\Omega)\,\mathrm{d}\Omega \qquad \frac{L}{P_L} \ll 1 \tag{7}$$

$$\sigma_p = \frac{L}{8P_L}\int\left[\nabla g(\Omega)\right]^2/g(\Omega)\,\mathrm{d}\Omega - 2\ln\int\left[g(\Omega)\right]^{1/2}\mathrm{d}\Omega \qquad \frac{L}{P_L} \gg 1 \tag{8}$$

For the rigid fibers, $g(\Omega)$ represents the distribution of particle orientations. Note that in the limit $(L/P_L) \to 0$, the orientational free energy reduces to Onsager's expression for rigid rods. For the long fibers, $g(\Omega)$ represents the distribution of segment orientations and ∇ is the gradient with respect to the fiber director, $\hat{n}$. Note that $g(\Omega)$ is normalized such that $\int \mathrm{d}\Omega\, g(\Omega) = 1$.

In previous studies of monodisperse systems [11,19,14,16,17], the limiting expressions for the free energy were interpolated to determine the orientational free energy for $L/P_L \approx 1$ and a trial function was used to describe the orientational distribution, $g(\Omega)$. For polydisperse systems, it is necessary to make further approximations. In this study, we model protein filaments that grow cooperatively such that the average fiber length is on the order of P_L. Comparing the above limiting expressions for σ_p to Hentschke's interpolated expression [14], we found that the limit of $L/P_L \gg 1$ (Eq. 8) is adequate to describe the flexibility effects in such systems (For $L/P_L = 1.0$, the error is 2–5%). We further simplify our calculation by only using the leading term

$$\sigma_p = \frac{L}{8P_L}\int\frac{\left[\nabla g(\Omega)\right]^2}{g(\Omega)}\mathrm{d}\Omega \tag{9}$$

(i.e., ignoring end-effects). Tests of this expression for $L/P_L = 1.0$ find that it underestimates Hentschke's interpolation by less than 10%; for $L/P_L = 2.0$ the error is reduced to less than 5%.

For the isotropic phase $g(\Omega) = 1$, and σ_p is

accordingly zero. To calculate σ_p for the nematic phase we use Onsager's trial distribution function,

$$g(\Omega) = \frac{\alpha}{\sinh(\alpha)}\cosh[\alpha\cos(\theta)] \tag{10}$$

where θ is the angle with respect to the director, and α is a parameter determined by minimizing the free energy. Substitution of the trial function into Eq. 9 yields

$$\sigma_p = \frac{L}{8P_L}\left[2\alpha\coth(\alpha) - 2 - \frac{\alpha^2\tan^{-1}(\sinh(\alpha))}{\sinh(\alpha)} + \frac{1}{\sinh(\alpha)}\int_0^\alpha x^2\,\mathrm{sech}(x)\,\mathrm{d}x\right] \tag{11}$$

The earlier assumption that the average fiber length is on the order of P_L allows us to assume that there is little correlation between the orientations at the two ends of any filament and that therefore α is independent of the filament length. Using the relation $L = (4a/3)(n-1)$ (see Fig. 1), the contribution to the free energy due to the orientational entropy of all particles is simply the sum of the single particle free energy terms

$$f_{\text{orient}} = \sum_{j,n} c_{jn}\frac{a_j(n-1)}{6P_L}\left[2\alpha_j\coth(\alpha_j) - 2 - \frac{\alpha_j^2\tan^{-1}(\sinh(\alpha_j))}{\sinh(\alpha_j)} + \frac{1}{\sinh(\alpha_j)}\int_0^{\alpha_j} x^2\,\mathrm{sech}(x)\,\mathrm{d}x\right] \tag{12}$$

where α_j is the orientation distribution parameter for filaments of type j.

2.3. Interparticle interactions

Since the bending of filaments occurs on the scale of the persistence length while interaction between particles occur on a length scale comparable to the filament diameter, particles 'see' only straight segments of each other and bending need not be considered in the calculation of the free energy due to interparticle interactions. As is conventional in treating crowded solutions, the solvent is treated as a continuum background mediating effective interactions between solute particles. Thus the need to describe van der Waals attractions between all types of species is avoided and only repulsions between solute particles are treated explicitly (see, e.g., Ref. [5]). Here we include only pure hard-core repulsions (excluded volume) because soft repulsions are insignificant in the case of electrically neutral semiflexible fibers. The most accurate closed form expression for the free energy due to excluded volume interactions among polydisperse particles is that given by scaled particle theory [20]

$$f_{\text{inter}} = -c_p\ln(1-v_p) + \frac{B}{2(1-v_p)} + \frac{C}{3(1-v_p)^2} \tag{13}$$

where

$$v_p = \sum_{jn} c_{jn}\frac{4}{3}\pi a_j^3 n \tag{14}$$

is the total particle volume fraction, a_j is the radius of a monomer of type j,

$$B = \sum_{jn}\sum_{j'n'} c_{jn}c_{j'n'}a_j a_{j'}\pi\left[4(a_j + a_{j'}) + \frac{4}{3}(2a_j + a_{j'})(n-1) + \frac{4}{3}(a_j + 2a_{j'})(n'-1) + \frac{8}{9}(a_j + a_{j'})(n-1)(n'-1)\rho_{jj'}\right] \tag{15}$$

and

$$C = DE \tag{16}$$

where

$$D = \sum_{jn} c_{jn}\left[\frac{4\pi a_j^2}{3}\right](2n+1),$$

$$E = \sum_{jn}\sum_{j'n'} c_{jn}c_{j'n'}a_j^2 a_{j'}^2\pi\left[2 + \frac{4}{3}(n-1) + \frac{4}{3}(n'-1) + \frac{8}{9}(n-1)(n'-1)\rho_{jj'}\right] \tag{17}$$

and

$$\rho_{jj'} = \frac{4}{\pi}\int\int \mathrm{d}\Omega \mathrm{d}\Omega' g_j(\Omega)\, g_{j'}(\Omega')\sin\gamma \qquad (18)$$

where $g_j(\Omega)$ and $g_{j'}(\Omega')$ represent the orientational distributions of the j and j' aggregates, respectively, and γ is the angle between the two interacting particles, or particle segments.

The configuration integral, ρ, for the hard-core interactions is equal to unity in the isotropic phase. In the nematic phase it is necessary to substitute Onsager's trial distribution function for $g(\Omega)$ to obtain

$$\rho_{jj'} = \frac{4}{\pi}\int\int \frac{\alpha_j \cosh(\alpha_j \cos\theta_j)\,\alpha_{j'}\cosh(\alpha_{j'}\cos\theta_{j'})}{\sinh(\alpha_j)\sinh(\alpha_{j'})} \times \sin\gamma \mathrm{d}\Omega \mathrm{d}\Omega' \qquad (19)$$

Following Onsager [5], this double integral can be simplified into the following single integral:

$$\rho = \frac{2}{\pi}\int_0^{\pi} \frac{\cosh\left[\left(\alpha_j^2 + \alpha_{j'}^2 + 2\alpha_j\alpha_{j'}\cos\gamma\right)^{1/2}\right]}{\sinh(\alpha_j)\sinh(\alpha_{j'})} \times \cos\gamma \mathrm{d}\gamma \qquad (20)$$

If the two particles are of the same species, $j = j'$, then $\alpha_j = \alpha_j' = \alpha$, and the exact solution is $\rho = 2I_2(2\alpha)/\sinh^2(\alpha)$ where I_2 is the modified Bessel function. When $j \neq j'$ ($\alpha_j \neq \alpha_j'$) then Eq. 20 has to be calculated numerically using a Gaussian quadrature method.

2.4. Equilibrium

A specific state of the system is described by the size distribution c_{jn} and segment orientation parameter α_j for filaments of each type j. The equilibrium state is that which has the lowest free energy. Accordingly, we minimize

$$\tilde{f}(\{c_{jn}, \alpha_j\}) = f(\{c_{jn}, \alpha_j\}) - \sum_j \left[\frac{\chi_j}{kT}\right] v_j(\{c_{jn}\}) \qquad (21)$$

with respect to $\{c_{jn}, \alpha_j\}$, where $v_j = \sum_n c_{jn}\frac{4}{3}\pi a_j^3 n$, is the total volume fraction of solute j and $\chi_j = \mu_j^0 - \mu_{\text{solvent}}^0$ is the conjugate Lagrange multiplier, equal to the difference in chemical potential between solute j and the implicit solvent. The minimization condition

$$\left.\frac{\partial(\tilde{f})}{\partial c_{jn}}\right|_{V,T,c_{j'n'}\neq c_{jn},\alpha_j} = 0 \qquad (22)$$

determines that the particle distribution has the form

$$c_{jn} = C_j P_j^{n-1} \qquad (23)$$

Note that for non-assembling species, P_j will be zero. After substituting Eq. 23 into Eq. 21, the equilibrium calculation is then completed for given values of all χ_j, by numerical minimization with respect to all C_j, P_j and α_j. The equilibrium values of these parameters can then be used to calculate macroscopic properties of interest, such as the volume fractions of each species, the average filament length for each species and the orientational ordering of each species.

3. Results

Whereas the compositions of binary systems are conventionally specified by points on a line, the compositions of ternary systems are conventionally represented by points in an equilateral triangle. The vertices of the triangle each represent a pure sample of one of the three species. In general, the fraction of a species decreases with distance from the corresponding vertex. Specifically, if a line is drawn from a vertex to the opposite leg, the fraction of the corresponding species decreases linearly with distance, from 1 at the vertex to 0 at the opposite leg. The virtue of an equilateral triangle is that for any point in the triangle, the fractions for the three species, calculated using lines through the three vertices, add up to 1. Note that all points on a line parallel to a leg of the triangle have the same fraction of the species represented by the opposing vertex. All points on a line through a given vertex have a constant ratio of the two species represented by the other two vertices. In this plane, information about the system can be displayed. Here we show the boundaries of regions with homogeneous solutions and regions with phase separation. In the two-phase regions we show tie-lines that indicate the composi-

tions of the coexisting phases. By the Gibb's phase rule, ternary diagrams can have up to three distinct phases coexisting at a given composition. However, we have not found such states in this study.

In Figs. 2–7 pure solvent is represented by the apex of the triangle (*). Of the two solutes, one reversibly self-assembles into filaments ($j = A$) and the other is either non-aggregating globular protein ($j' = B$) or also reversibly self-assembles into filaments ($j' = A'$). In all cases, the aggregating species have been assigned association energies of $\phi_0 = 32$ and $\phi_c = -5$ to polymerize cooperatively at low concentrations, as cytoskeletal proteins do. The effects of varying the strength of association have been considered earlier [2].

3.1. Mixtures of filament forming protein and non-aggregating globular protein

Figs. 2–4 show the behavior of mixtures of a reversibly self-assembling species ($j = A$) and a non-aggregating species ($j' = B$) in solvent (*). For the present purposes, the diameters of both solutes are taken to be the same. The difference between the figures is in the persistence lengths of the filaments.

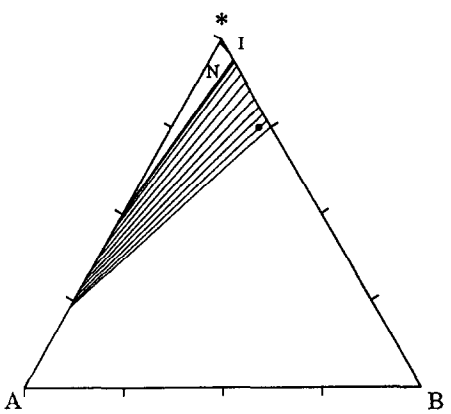

Fig. 2. Ternary phase diagram for cooperatively self-assembled rigid filaments (A) and a non-aggregating species (B) with the same diameter in solvent (*). The results are obtained using Madden & Herzfeld's model [2] for rigid filaments with weak, soft repulsive interactions ($J = 0.25$ and $\xi = 0.05$), modified to incorporate cooperativity in filament assembly. N and I indicate homogeneous nematic (i.e., orientationally ordered) and isotropic solutions, respectively. In the two-phase region, tie lines connect coexisting isotropic and nematic solutions. The dot represents the typical composition of a cell.

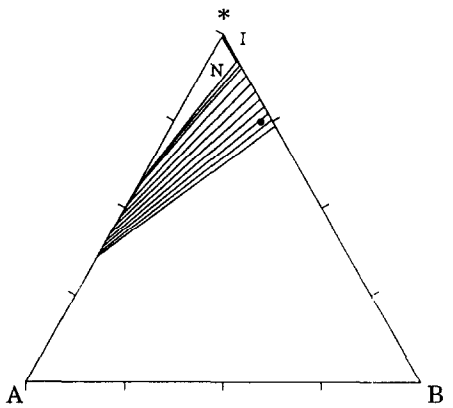

Fig. 3. Ternary phase diagram for cooperatively self-assembled semi-flexible filaments (A) with (P_L/a) = 2000 and a non-aggregating species (B) with the same diameter in solvent (*). N and I indicate homogeneous nematic (i.e., orientationally ordered) and isotropic solutions, respectively. In the two-phase region, tie lines connect coexisting isotropic and nematic solutions. The dot represents the composition of a typical cell.

Fig. 2 shows the behavior for perfectly rigid filaments (infinite persistence length) calculated using the theory of Madden and Herzfeld [2] with the present cooperative free energy of filament assembly (Eqs. 3 and 4). Figs. 3 and 4 show the behavior for semi-flexible filaments with relative persistence length (P_L/a) = 2000 (comparable to actin filaments [10]) and 200 (comparable to poly-γ-benzyl-L-glutamate [21]), respectively. In all three cases, the most dilute solutions (near the apex of the triangle) and all solutions devoid of filament forming protein (along the right leg) are isotropic as expected. As also expected, concentrated solutions of filament forming protein (down the left leg) form a single nematic (i.e., orientationally ordered) phase and, the more flexible the filaments, the higher the concentration required to induce alignment (compare the transition at ~2 vol.-% in Fig. 3 vs. ~8 vol.-% in Fig. 4). The same effect of flexibility in binary self-assembling systems has been reported by Hentschke [18] using different modeling assumptions. For mixtures approximating the composition of cells (~25 vol.-% solute, of which ~10% is filament forming and ~90% is non-aggregating — marked on the diagrams by a dark dot) dramatic demixing occurs. This separation of dense filament bundles was reported previously for rigid, non-cooperatively assem-

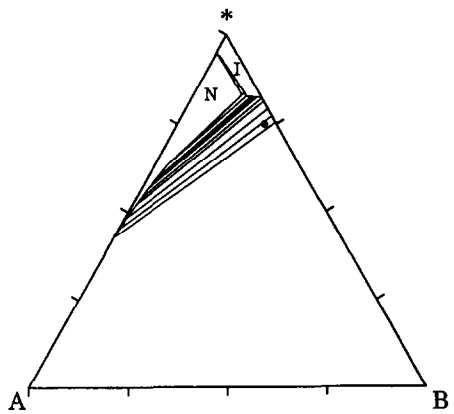

Fig. 4. As in Fig. 3 except $(P_L/a) = 200$.

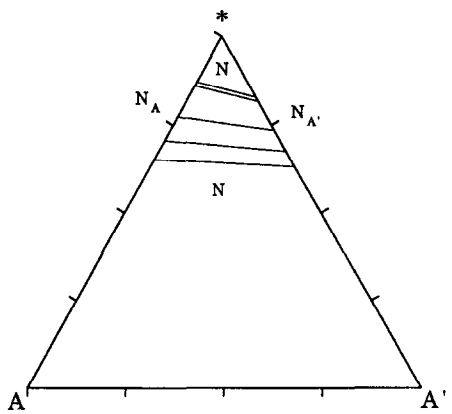

Fig. 5. Ternary phase diagram of two reversibly self-assembling, semi-flexible filaments (A and A') in solvent (*). Both solutes have the same diameter ($a = a'$) but, whereas the relative persistence for length A is $(P_L/a) = 2000$, the relative persistence length for A' is $(P'_L/a') = 20000$. The tie lines connect coexisting nematic phases, N_A and N'_A and N represents a single nematic phase containing A and A'.

bled filaments [2]. The main effect of filament flexibility is that the coalesced filaments are less tightly packed (lower end of the tie-line at ~75 vol.-%, ~60 vol.-% and ~55 vol.-% in Figs. 2–4, respectively). The other significant difference between Fig. 3 and Fig. 4 is that the nematic region extends further into the triangle with increasing filament flexibility. This indicates that the more flexible filaments more readily accommodate interspersed B particles. However, these concentrations are not of physiological significance.

3.2. Mixtures of two types of self-assembling proteins forming filaments with different flexibilities

Since both flexible and rigid filaments demix from globular proteins, the question arises as to whether, when both types of filaments occur in the same system, they will coalesce separately or together.

Figs. 5–7 show the behavior of mixtures of two reversibly self-assembling species ($j = A$, $j' = A'$) in solvent (*). In Fig. 5, the aggregating species have the same diameter ($a = a'$), but different relative persistence lengths [$(P_L/a) = 2000$ and $(P'_L/a') = 20000$]. In Fig. 6, the diameters are different ($a' = 4a$) but the relative persistence lengths are the same [$(P_L/a) = (P'_L/a') = 2000$]. In Fig. 7 the proteins differ both in diameter ($a' = 4a$) and in relative persistence lengths [$(P_L/a) = 2000$ and $(P'_L/a') = 2500$]. This last system is parametrized to approximate a mixture of thin, flexible actin filaments and stiffer, thicker microtubules.

On the scale of these diagrams, the isotropic phase which is present at low solute concentrations is not visible. At the semi-dilute concentrations visible near the apex of the triangles, a single nematic is formed. Thus, whether aligned or not, filaments of different flexibilities mix freely when packing is not too tight. However, at higher concentrations, fila-

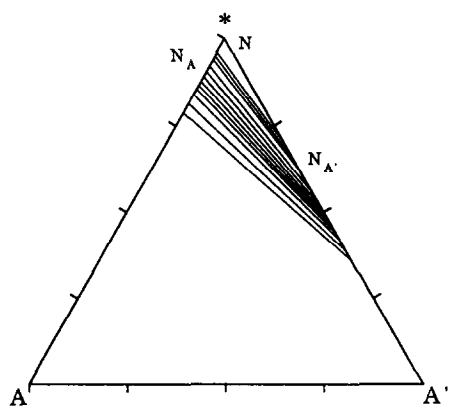

Fig. 6. As in Fig. 5, except that A' has a 4-fold larger diameter ($a' = 4a$) and a somewhat shorter persistence length so that the relative persistence length is the same for both A and A' [$(P_L/a) = (P'_L/a') = 2000$].

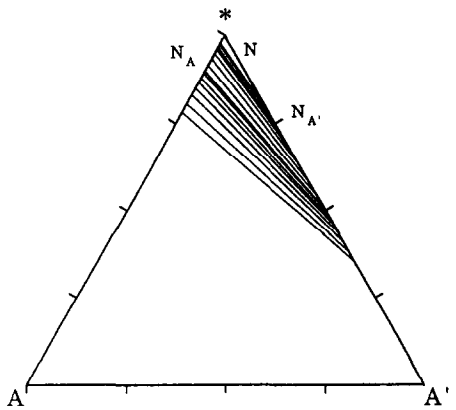

Fig. 7. As in Fig. 6 except that $(P_L'/d') = 2500$ so that A' approximates the properties of microtubules while A approximates the properties of actin microfilaments.

ments segregate completely into two essentially pure nematic phases. The tilt of the tie-lines shows that solvent partitions somewhat preferentially with the more flexible filaments (Fig. 5) and strongly preferentially with the more numerous thinner filaments (Figs. 6 and 7). This reflects the fact that more entropy is gained by diluting the solute that has more degrees of freedom. At still higher concentrations, where packing constraints force even the more flexible filaments to straighten out, filaments again mix in a single nematic phase when they have the same diameter (see Fig. 5). However, when the stiffer filaments are fatter (Figs. 6 and 7), there is no sign of reentry into a single nematic, even at the highest numerically tractable concentrations.

4. Discussion

The present study was intended to address two questions. The first is whether the spontaneous bundling predicted for rigid filaments in the presence of high concentrations of globular proteins [2] persists when filament flexibility is taken into account. Figs. 3 and 4 show that bundling occurs even for filaments as flexible as poly-γ-benzyl-L-glutamate. This is not surprising because even with a relative persistence length as small as $(P_L/a) = 200$, the filaments are essentially straight over lengths considerably longer than the widths of the globular proteins. Therefore the rod-sphere packing problem, due to the wasted space when spheres are interspersed between rods, is nearly as severe for the flexible filaments as for the rigid ones. The theoretical prediction of crowding-induced bundling of flexible filaments is consistent with experimental observations of spontaneous filament bundling in mixtures of F-actin and high molecular weight globular molecules [3,4].

Comparison of Figs. 3 and 4 shows that the main effect of filament flexibility on bundling is to cause somewhat looser packing. In previous work, it has been shown that the density of filament bundles is also affected by the diameter of the filaments: the thicker the filaments relative to the diameter of the globular protein, the tighter the filament bundles [2]. Thus, for cytoskeletal filaments, the thickness of the stiffer microtubules, compared to the thinness of the more flexible actin filaments, would accentuate differences in the densities of the bundles that each would form in the presence of the same globular proteins.

The second question motivating the present work is whether filaments with different flexibilities will bundle together or separately. This is actually a question about quaternary systems (two filament forming solutes and a non-aggregating globular solute in solvent). However some insight can be obtained by examining the ternary systems in Figs. 5–7. Generally, above a certain concentration, filaments with different flexibilities separate. This occurs because the orientational freedom gained by the segments of the flexible filaments and the translational freedom gained by the rigid filaments exceeds the loss of mixing entropy. However, when the concentration gets so high that packing forces the more flexible filaments to be as straight as the rigid ones, then mixing can recur. This is seen for filaments with equal width in Fig. 5. With increasing concentration, the packing of the two coexisting phases becomes more and more comparable (i.e., the tie-lines lie flatter indicating similar solvent contents in the two phases) and mixing recurs at ~ 37 vol.-% solute. Thus at the densities of the bundles formed in the presence of physiological levels of globular protein (Figs. 3 and 4), filaments with equal widths (Fig. 5) are mixed. However, when the diameters

differ by a factor of 4 (Figs. 6 and 7), the packing of the two coexisting phases is still very different at the highest numerically tractable concentrations (i.e., the tie-lines are still very steep indicating very different solvent contents in the two phases). This suggests that such filaments will spontaneously form segregated bundles in the presence of physiological levels of globular protein.

The relative persistence lengths and diameters of the model filaments in Fig. 7 were chosen to approximate those of F-actin and microtubules. The results suggest that these filaments can form segregated bundles in cells without the assistance of cross-linking proteins. The comparison with Figs. 5 and 6 shows that the accentuated segregation in the F-actin/microtubule system is due to the fact that the more flexible filaments are also narrower. Thus the coincidence of shorter filament persistence length with smaller filament diameter may have functional significance.

The conclusion that free filaments form bundles spontaneously under crowded conditions, is contrary to the conventional wisdom that cross-linking proteins are necessary for bundle formation. In fact, it appears that cross-linking proteins serve more subtle purposes. While, the chemical specificity of cross-linkers can help to stabilize the segregation of filaments into separate bundles, cross-linkers with the appropriate geometric specificity can induce greater regularity in filament bundles by preferentially stabilizing the polarity and registration of filaments. Thus cross-linkers may be more important for fine tuning bundle structure than for the bundling itself. On the other hand, it is possible that cross-linkers with a contrary geometric specificity can frustrate bundling by stabilizing orthogonal contacts between filaments to generate an isotropic gel.

Acknowledgements

This work was facilitated by helpful discussions with Thomas L. Madden, Olga Kheifets and Jining Han. We are also grateful for the advice of Alan E. Berger regarding the evaluation of Eq. 20. This work was supported by NIH grant HL36546.

References

[1] J. Darnell, H. Lodish and D. Baltimore, Molecular Cell Biology, Scientific American Books, New York, 1986.
[2] T.L. Madden and J. Herzfeld, Biophys. J., 65 (1993) 1147.
[3] A. Suzuki, M. Yamazaki and T. Ito, Biochemistry, 28 (1989) 6513.
[4] P. Cuneo, E. Magri, A. Verzola and E. Grazi, Biochem. J., 281 (1992) 507.
[5] L. Onsager, Ann. N.Y. Acad. Sci., 51 (1949) 627.
[6] M.P. Taylor, R. Hentschke and J. Herzfeld, Phys. Rev. Lett., 62 (1989) 800.
[7] R. Hentschke, M.P. Taylor and J. Herzfeld, Phys. Rev. A, 40 (1989) 1678.
[8] M.P. Taylor and J. Herzfeld, Phys. Rev. A, 43 (1991) 1892.
[9] T.L. Madden and J. Herzfeld, J. Cell Biol., 126 (1994) 169.
[10] E.H. Egelman and D.J. DeRosier, J. Mol. Biol., 217 (1991) 405.
[11] T. Odijk, J. Phys., Paris, 48 (1987) 125.
[12] A.R. Khokhlov and A.N. Semenov, Physica A, 108 (1981) 546.
[13] A.R. Khokhlov and A.N. Semenov, Physica A, 112 (1982) 605.
[14] R. Hentschke, Macromolecules, 23 (1990) 1192.
[15] R. Hentschke and J. Herzfeld, Phys. Rev. A, 44 (1991) 1148.
[16] D.B. DuPre and S-J. Yang, J. Chem. Phys., 94 (1991) 7466.
[17] T. Sato, T. Shoda and A. Teramoto, Macromolecules, 27 (1994) 164.
[18] R. Hentschke, Liquid Cryst., 10 (1991) 691.
[19] T. Sato, N. Ikeda, T. Itou and A. Teramoto, Polymer, 30 (1989) 311.
[20] M.A. Cotter and D.C. Wacker, Phys. Rev. A, 18 (1978) 2676.
[21] M. Schmidt, Macromolecules, 17 (1984) 553.